Self-consistent analysis of fundamental and higher harmonic ICRF heating in tokamak plasmas

Hideo Nuga, Atsushi Fukuyama

Department of Nuclear Engineering, Kyoto University, Kyoto 606-8501, Japan

(Received: 3 September 2008 / Accepted: 20 November 2008)

The deviation of the distribution functions from the Maxwellian due to the interaction with waves affects the propagation and absorption of the wave itself. Therefore self-consistent analysis including the modification of the momentum distribution function is required for quantitative analysis of wave heating and current drive. The modeling code TASK was updated to describe the momentum distribution function of multi-species and the wave dielectric tensor for arbitrary momentum distribution function. Numerical results of ICRF heating in tokamak plasmas which generate energetic tail of distribution function are reported for minority heating and the second harmonic heating.

Keywords: ICRF, Heating, Simulation, Integrated code

1. Introduction

Plasma heating and current drive by RF waves deform the momentum distribution function of heated species. The deviation of the distribution functions from the Maxwellian affects the propagation and absorption of the wave itself. Therefore self-consistent analysis including the modification of the momentum distribution function is required for quantitative analysis of wave heating and current drive.

Self-consistent analysis of electron cyclotron current drive (ECCD) using ray tracing method has already been achieved by the integrated tokamak modeling code TASK. The purpose of this study is to develop full wave analysis of ICRF simulation including the deformation of distribution function. In this paper, results of ICRF heating analysis in tokamak plasma using the integrated code TASK are reported.

The full wave component TASK/WM [1] calculates the wave electric field by solving Maxwell's equation including the plasma dielectric tensor. The bounce-averaged Fokker-Planck component TASK/FP analyze the time evolution of the momentum distribution functions for electrons and ions by solving the Fokker-Planck equation including the quasi-linear diffusion terms calculated from the wave electric field. The dielectric tensor component TASK/DP calculates the plasma dielectric tensor by numerically integrating the momentum distribution functions. By repeating this cycle, we can describe the time evolution or the steady state of the wave heating and current drive.

In the case of minority heating by ICRF waves, energetic minority ions are generated at the fundamental cyclotron resonance and a high-energy tail of the minority momentum distribution function which affects the absorption of the ICRF waves is formed. In the case of second cyclotron harmonics, a small fraction of ions is strongly accelerated and stronger energetic tail is generated. In both cases, the electron momentum distribution function is flattened in the vicinity of the parallel wave-particle resonance and the modification leads to the power absorption through the Landau damping or TTMP as well as the current drive.

We have carried out numerical analysis of ICRF heating and confirmed that the modification of momentum distribution function from Maxwellian affects the deposition to ions. Both the cases of minority heating and second harmonic resonance heating are reported.

2. Model of Fokker-Planck analysis

First, we describe the Fokker-Planck module, TASK/FP, which solves the bounce averaged Fokker-Planck equation.

$$\frac{\partial f_s}{\partial t} = E(f_s) + C(f_s) + Q(f_s) + L(f_s) + S(f_s) \tag{1}$$

where the terms E, C, Q, L, and S are acceleration term by the toroidal DC electric field, collision term due to Coulomb collision, quasi-linear diffusion term due to wave-particle interaction, spatial diffusion term and source term, respectively. f_s denotes the momentum distribution function for species s, $f_s(p_\parallel, p_\perp, \rho, t)$ where $p_\parallel$ and $p_\perp$ are the parallel and perpendicular momentam at the minimum magnetic field point on the magnetic surface and ρ is the normalized minor radius of the surface. L and S terms are not included in the present analysis.

FP module includes the trapped particle effect by bounce averaging with zero banana width. This module can calculate time evolution of distribution functions not only for mainly heated species but also for the other species all together.

FP modules solve the Fokker-Planck equation as a diffusion equation.

$$\frac{\partial f_s}{\partial t} = -\nabla_p \cdot \left(-\overleftrightarrow{D} \cdot \nabla_p f_s + \boldsymbol{F} f_s \right) \tag{2}$$

author's e-mail: nuga@p-grp.nucleng.kyoto-u.ac.jp

where $\overleftrightarrow{D}$ and $\boldsymbol{F}$ are diffusion and friction coefficients. Each coefficients are composed of several terms, e.g. [2]

$$\overleftrightarrow{D} = \overleftrightarrow{D}_{\rm cl} + \overleftrightarrow{D}_{\rm ql}$$
$$\boldsymbol{F} = \boldsymbol{F}_{\rm cl} + \boldsymbol{F}_{\rm dc}.$$

The subscripts "cl", "ql" and "dc" denote collision, quasi-linear and DC electric field acceleration, respectively.

Several models for Coulomb collision terms ($\overleftrightarrow{D}_{\rm cl}$ and $\mathbf{F}_{\rm cl}$) are available in the FP module. The linear collision model [2] assumes the Maxwellian distribution for field particles. It doesn't conserve the total momentum or energy and is not adequate when various heating processes occur simultaneously. In the non-linear collision model [2-4], the distribution functions of field particle species are expanded by the Legendre polynomials $P_l(\cos\theta)$ as,

$$f_s(\boldsymbol{v}_s) = \sum_{l=0}^{L} f_s^{(l)}(v_s) P_l(\cos\theta_s) \tag{3}$$

where θ is a pitch angle at the minimum magnetic field point on the magnetic surface. By integration over v_s, we can calculate the non-linear collision terms. If we keep the lowest order term ($L = 0$), the non-linear term conserves only the particle number. The non-linear Coulomb collision model satisfies momentum ($L \geq 1$) and energy ($L \geq 2$) conservation. Relativistic effect is also included according to the formulation by Braams [4].

The quasi-linear term is purely diffusive. Expression of the quasi-linear diffusion term is given by [2]

$$\overleftrightarrow{D}_{\rm ql} = \sum_n \frac{\pi}{2} \frac{q_s^2}{m_s^2} \delta(\omega - k_\parallel v_\parallel - n\Omega_s/\gamma) \boldsymbol{a}_n^* \boldsymbol{a}_n \tag{4}$$

where

$$\boldsymbol{a}_n = \Theta_n \frac{k_\parallel}{\omega} \left[\left(\frac{\omega}{k_\parallel} - v_\parallel \right) \boldsymbol{v}_\perp + v_\perp \boldsymbol{v}_\parallel \right]$$
$$\Theta_n = \frac{E_{\rm w+} J_{n-1} + E_{\rm w-} J_{n-1}}{\sqrt{2}} + \frac{v_\parallel}{v_\perp} J_n E_{\rm w\parallel}$$

when ω_s, $k_\parallel$, $k_\perp$, Ω, γ are the wave frequency, the parallel and perpendicular wave numbers, the cyclotron frequency and the relativistic factor, respectively. J_n is the Bessel function $J_n(k_\perp v_\perp/\Omega_s)$. Wave electric field $E_{\rm w\pm}$ and $E_{\rm w\parallel}$ are calculated by the full wave analysis code TASK/WM.

3. Verification of the non-linear collision term

To numerically verify our model, we compare the electrical conductivity calculated by our model with that in Karney's previous work [2]. These are tabulated in table I (non-relativistic) and II (relativistic). In all cases, we use non-linear electron electron collision term and the electron-ion collision operator is given by an approximate formula [2].

In table I, we used non-relativistic, non-linear (momentum conserving) model for electron-electron collision and approximate model for electron-ion collision with the electric field $E = 0.001$ V/m. Table II shows electrical conductivity for the relativistic model with $E = 0.001$ V/m and $\Theta = T_e/m_e c^2 = 0.02$. Since the agreement in the both tables is fairly good, validity of conductivity of our model is confirmed.

model	$Z_i = 1$	$Z_i = 2$	$Z_i = 5$	$Z_i = 10$
linearized [2]	7.429	4.377	2.078	1.133
our model	7.341	4.310	2.038	1.108

Table I The electrical conductivity for various ion charge. The conductivities are normalized to $n_e q_e^2/m_e \nu_{te}$.

model	$Z_i = 1$	$Z_i = 2$	$Z_i = 5$	$Z_i = 10$
linearized [2]	7.160	4.180	1.963	1.064
our model	7.250	4.283	2.035	1.111

Table II The electrical conductivity for various ion charge. The conductivities are normalized to $n_e q_e^2/m_e \nu_{te}$.

4. Calculation results

We carried out numerical analysis of ICRF heating in two cases. In these analyses, we used the parameters in table III simulating JT-60U like tokamaks.

major radius	R_0	3.5m
minor radius	a	0.98m
elongation	κ	1.28
triangularity	δ	0.31
magnetic field on axis	B_0	3.3T
temperature on axis	T_0	4.0keV
temperature on surface	T_s	0.4keV
density on axis	n_0	$0.3\times10^{20}/\mathrm{m}^3$
density on surface	n_s	$0.3\times10^{19}\mathrm{m}^3$
minority ion ratio		5%
frequency	f_{RF}	55.0MHz
toroidal mode number	n_ϕ	16 ~ 24
number of poloidal mode	N_θ	32 ~ 64

Table III Plasma parameters

4.1 Minority heating

First, we studied the case of ICRF heating of plasmas composed of two ion species, majority deuteron 95% and minority proton 5%. In this analysis, the total heating power is 1.50 MW, and the wave absorption power to electron, deuteron and proton are 0.37, 0.07 and 1.06 MW. In this plasma, minority ion is mainly accelerated by the ion cyclotron fundamental resonance. Fig.1 (a) shows radial profile of wave absorption by mostly protons, and (b) shows the profile of the wave deposition power density to protons on the poloidal cross section. Most of the wave power is absorbed by the minority ions on funda-

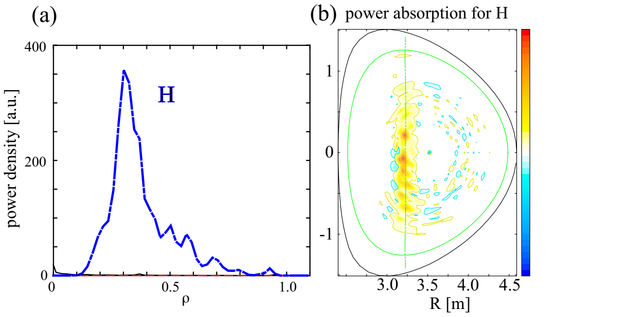

Fig. 1 (a) Radial profile of wave absorption calculated by WM. (b) Wave absorption profile for proton on the poloidal cross section.

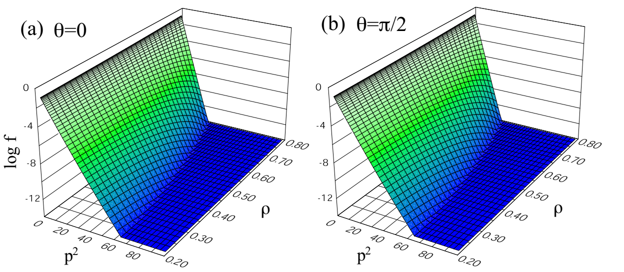

Fig. 2 Electron distribution function for parallel and perpendicular 1D momentum space at various radial positions.

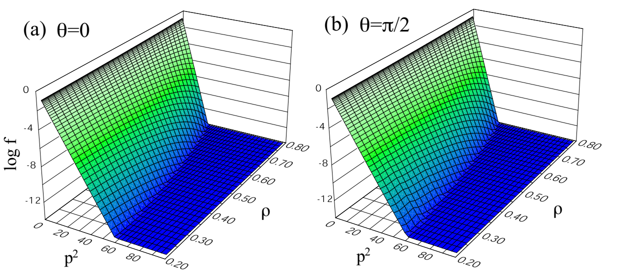

Fig. 3 Deuteron distribution function for parallel and perpendicular 1D momentum space at various radial positions.

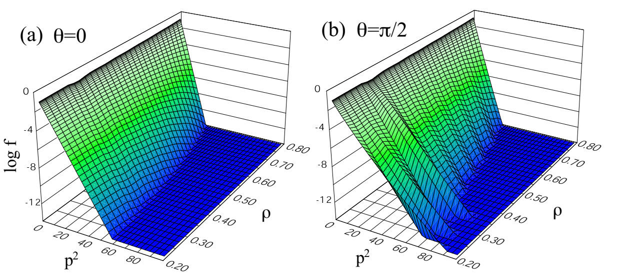

Fig. 4 Proton distribution function for parallel and perpendicular 1D momentum space at various radial positions.

mental absorption resonance surface. Figs.2 - 4 indicate the distribution function in the parallel (a) and perpendicular (b) momentum direction. Fig.2 and 3 show that the electron and deuteron distribution functions are isotropic, while Fig.4 indicates that proton distribution function is anisotropic. Radial profiles of wave power absorption and power transfer through collision at 5 msec after the onset

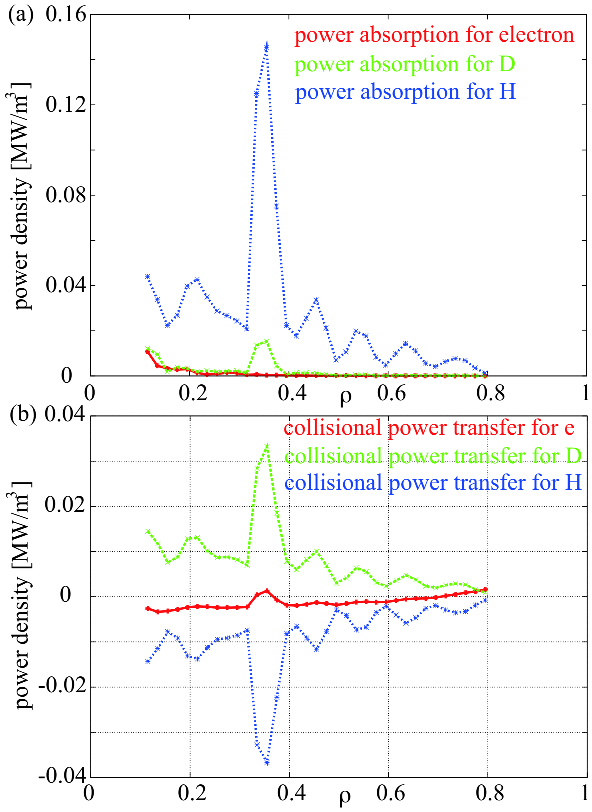

Fig. 5 (a) Radial profile of the wave power absorption. (b) Radial profile of the power transfer through collision.

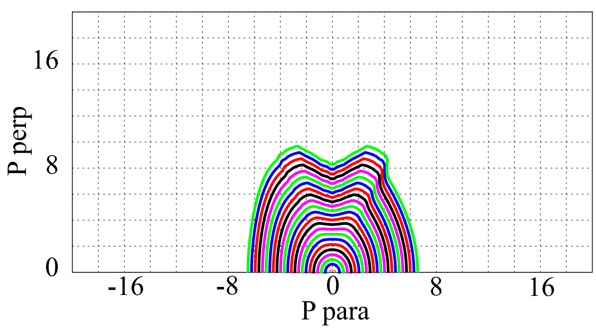

Fig. 6 Contour of proton distribution function at $\rho = 0.35$ in 2D momentum space.

of wave heating are shown in Fig.5. From this figure, we confirmed that minority ions are heated by ICRF waves, while majority ions are heated by collisions with minority ions. The collisional power gain of deuteron almost balances with the collisional power loss of proton. On the other hand, electrons are rarely heated by waves and collision except at $\rho = 0.35$ where electrons are slightly heated by collisions with minority ions. From Fig.5, we see that the power absorption from wave is greater than the power loss due to collisional power transfer to the minority ions. The difference of the power is attributed to the increase of the tail ions because the tail formation is not saturated yet. We note that the electrons absorb the wave power at the

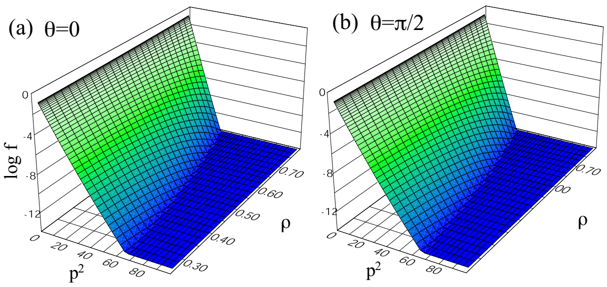

Fig. 7 Electron distribution function for parallel and perpendicular 1D momentum space at various radial positions.

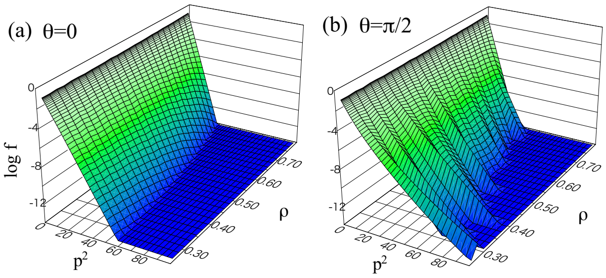

Fig. 8 Deuteron distribution function for parallel and perpendicular 1D momentum space at various radial positions.

Alfvén resonance near the plasma surface due to the relativity large $k_{\|}$ for $n_\phi = 24$.

Fig. 6 is a contour of minority ion distribution function at the normalized minor radius $\rho = 0.35$ in 2D momentum space. Minority ions are heated strongly at $\rho = 0.35$ as depicted in Fig.5. Contour of the distribution function in Fig. 6 has two tips. These strongly accelerated pitch angles are the result of trapped particle effect. When reflecting point of a trapped particle coincide with a cyclotron resonance surface, this strong acceleration occurs, because such trapped particles stay at the resonance surface longer than passing particles. The pitch angle is $\pi/2$ when the resonant surface is tangential to the magnetic surface($\rho \sim 0.3$). In the present calculation, however, since the wave amplitude on the resonance surface is larger on the outer magnetic surface($\rho = 0.35$), the accelerated pitch angle deviates from $\pi/2$.

4.2 Second harmonic resonance

Next, the case of deuterium plasma was analyzed. In this plasma, ions are accelerated by the second harmonic resonance of 55 MHz ICRF wave. In the present analysis, the wave absorption power to electron and deuteron are 0.19 and 1.45 MW. Second harmonic resonance deforms the distribution function more strongly than the fundamental resonance. Figs.7 and 8 indicate the distribution function in the parallel (a) and perpendicular (b) momentum directions at 10 msec after the onset of wave heating . From Fig.7, we see that the electron distribution function stays isotropic. On the other hand, Fig. 8 shows strong deformation of the deuteron distribution function.

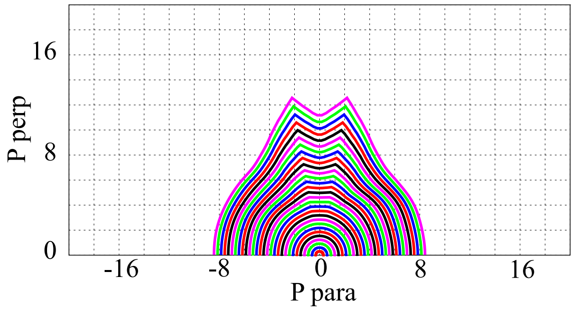

Fig. 9 Contour of the deuteron distribution function at $\rho = 0.33$ in 2D momentum space.

In the minority heating case, deuterons were heated by collision with wave heated minority ions. By contrast, in the second harmonic case, deuteron is heated by direct wave absorption. Since the absorption rate increases with the increase of $p_\perp$, strong tail is generated in the perpendicular direction and the distribution function becomes anisotropic.

Fig.9 shows the deformed deuteron distribution function in 2D momentum space at $\rho = 0.33$, where the wave absorption has a peak value. From Fig.9, we see that the deuteron distribution function has two tips as same as Fig.6.

5. Conclusion

We have updated the wave related modules in the TASK code for self-consistent analysis of ICRF heating in tokamak. The present numerical analysis describes the tail formation of the resonant ion momentum distribution function. We confirmed that deformation of distribution function occurs when the plasma is heated by waves. Self-consistent analysis required for quantitative analysis of wave heating and current drive is under way.

Acknowledgements This work was supported in part by the Grant-in-Aid for scientific research, Nos. 19360415 and 20226017, from Japan Society for the Promotion of Science (JSPS) and the Grant-in-Aid for specially-promoted research, No. 16002005, from Ministry of Education, Culture, Sports, Science and Technology (MEXT).

[1] FUKUYAMA, A., et al.: Proc. of 20th IAEA FEC (Villamoura, 2004) IAEA-CSP-25/CD/TH/P2-3.
[2] Charles F.F. Karney, Computer Physics Report **4**, 183 (1986)
[3] J. Killeen, G.D. Kerbel, M.G. McCoy, A.A. Mirin, *Computational Methods for Kinetic Models of Magnetically Confined Plasmas*, (Springer-Varlag, 1986)
[4] Bastiaan J. Braams and Charles F.F. Karney, Phys. Fluid B **1**, 1355 (1989)